

Third-harmonic generation via broadband cascading in disordered quadratic nonlinear media

W. Wang^{1,2}, V. Roppo^{1,3}, K. Kalinowski¹, Y. Kong², D. N. Neshev¹,
C. Cojocaru³, J. Trull³, R. Vilaseca³, K. Staliunas^{3,4}, W.
Krolikowski^{1*}, S. M. Saltiel^{1,5}, and Yu. Kivshar¹

¹Nonlinear Physics Center and Laser Physics Center, Research School of Physics and Engineering, Australian National University, Canberra ACT 0200, Australia

²College of Physics Science, Nankai University, Tianjin, 300071, China

³Departament de Física i Enginyeria Nuclear, Escola Tècnica Superior d'Enginyeries Industrial y Aeronàutica de Terrassa, Universitat Politècnica de Catalunya, Colom 11, 08222 Terrassa, Barcelona, Spain

⁴Institut Català de Recerca i Estudis Avançats (ICREA)

⁵Faculty of Physics, Sofia University, 5 J. Bourchier Blvd., BG-1164, Sofia, Bulgaria

wzk111@rsphysse.anu.edu.au

Abstract: We study parametric frequency conversion in quadratic nonlinear media with disordered ferroelectric domains. We demonstrate that disorder allows realizing *broadband third-harmonic generation* via cascading of two second-order quasi-phase matched nonlinear processes. We analyze both spatial and polarization properties of the emitted radiation and find the results in agreement with our theoretical predictions.

© 2009 Optical Society of America

OCIS codes: (190.0190) Nonlinear optics; (190.4420) Nonlinear optics: Nonlinear optics, transverse effects in; (190.2620) Harmonic generation and mixing

References and links

1. J. A. Armstrong, N. Bloembergen, J. Ducuing, and P. S. Pershan, "Interactions between Light Waves in a Non-linear Dielectric," *Phys. Rev.* **127**, 1918–1939 (1962).
2. P. A. Franken, and J. F. Ward, "Optical harmonics and nonlinear phenomena," *Rev. Mod. Phys.* **35** 23–39 (1963).
3. M. M. Fejer, G. A. Magel, D. H. Jundt, R. L. Byer, "Quasi-phase-matched 2nd harmonic-generation - tuning and tolerances," *IEEE J. Quantum Electron.* **28**, 2631–2654 (1992)
4. S. Zhu, Y. Y. Zhu, N. B. Ming, "Quasi-phase-matched third-harmonic generation in a quasi-periodic optical superlattice," *Science* **278**, 843–846 (1997).
5. U. K. Sapaev, G. Assanto, "Efficient high-harmonic generation in engineered quasi-phase matching gratings," *Opt. Express* **16**, 1–6 (2008).
6. M. Lu, X. F. Chen, "Multiple quasi-phase matching in engineered domain-inverted optical superlattice," *J. Non-linear Opt. Phys. Mater.* **16**, 185–198 (2007).
7. M. Horowitz, A. Bekker, B. Fischer, "Broad-band 2nd-harmonic generation in $\text{Sr}_x\text{Ba}_{1-x}\text{Nb}_2\text{O}_6$ by spread-spectrum phase-matching with controllable domain gratings," *Appl. Phys. Lett.* **62**, 2619–2654 (1993).
8. S. Kawai, T. Ogawa, H. S. Lee, R. C. DeMattei and R. S. Feigelson, "Second-harmonic generation from needle-like ferroelectric domains in $\text{Sr}_{0.6}\text{Ba}_{0.4}\text{Nb}_2\text{O}_6$ single crystals," *Appl. Phys. Lett.* **73**, 768–770 (1998).
9. M. Baudrier-Raybaut, R. Haidar, Ph. Kupecek, Ph. Lemasson, and E. Rosencher, "Random quasi-phase-matching in bulk polycrystalline isotropic nonlinear materials," *Nature (London)* **432**, 374–376 (2004).
10. P. Molina, M. O. Ramirez, and L. E. Bausa, "Strontium Barium Niobate as a Multifunctional Two-Dimensional Nonlinear Photonic Glass," *Adv. Funct. Mater.* **18**, 709–715 (2008).
11. J. J. Romero, D. Jaque, J. García Solé, and A. A. Kaminskii, "Simultaneous generation of coherent light in the three fundamental colors by quasicylindrical ferroelectric domains in $\text{Sr}_{0.6}\text{Ba}_{0.4}(\text{NbO}_3)_2$," *Appl. Phys. Lett* **81**, 4106–4108 (2002).

12. J. J. Romero, C. Aragó, J. A. Gonzalo, D. Jaque, and J. García Solé, "Spectral and thermal properties of quasiphase-matching second-harmonic generation in Nd³⁺:Sr_{0.6}Ba_{0.4}(NbO₃)₂ multi-self-frequency-converter nonlinear crystals," *J. Appl. Phys.* **93**, 3111–3113 (2003).
13. M. O. Ramirez, J. J. Romero, P. Molina, and L. E. Bausa, "Near infrared and visible tunability from a diode pumped Nd³⁺ activated strontium barium niobate laser crystal," *Appl. Phys. B* **81**, 827–830 (2005).
14. A. R. Tunyagi, M. Ulex, and K. Betzler, "Noncollinear optical frequency doubling in strontium barium niobate," *Phys. Rev. Lett.* **90**, 243901 (2003).
15. J. Trull, C. Cojocar, R. Fischer, S. M. Saltiel, K. Staliunas, R. Herrero, R. Vilaseca, D. N. Neshev, W. Krolikowski, and Yu. S. Kivshar, "Second-harmonic parametric scattering in ferroelectric crystals with disordered nonlinear domain structures," *Opt. Express* **15**, 15868–15877 (2007).
16. V. Roppo, D. Dumay, J. Trull, C. Cojocar, S. M. Saltiel, K. Staliunas, R. Vilaseca, D. N. Neshev, W. Krolikowski, and Yu. S. Kivshar, "Planar second-harmonic generation with noncollinear pumps in disordered media," *Opt. Express* **16**, 14192–14199 (2008).
17. R. Fischer, D. N. Neshev, S. M. Saltiel, W. Krolikowski, and Yu. S. Kivshar, "Broadband femtosecond frequency doubling in random media," *Appl. Phys. Lett.* **89**, 191105 (2006).
18. R. Fischer, D. N. Neshev, S. M. Saltiel, A. A. Sukhorukov, W. Krolikowski, and Yu. S. Kivshar, "Monitoring ultrashort pulses by the transverse frequency doubling of counterpropagating pulses in random media," *Appl. Phys. Lett.* **91**, 031104 (2007).
19. O. Pfister, J. S. Wells, L. Hollberg, L. Zink, D. A. VanBaak, M. D. Levenson, W. R. Bosenberg, "Continuous-wave frequency tripling and quadrupling by simultaneous three-wave mixings in periodically poled crystals: application to a two-step 1.19–10.71- μ m frequency bridge," *Opt. Lett.* **22**, 1211–1213 (1997).
20. S. M. Saltiel, A. A. Sukhorukov, Y. S. Kivshar, "Multistep parametric processes in nonlinear optics," *Prog. Opt.* **47**, 1–73 (2005).
21. N. Fujioka, S. Ashihara, H. Ono, T. Shimura, K. Kuroda, "Cascaded third-harmonic generation of ultrashort optical pulses in two-dimensional quasi-phase-matching gratings," *J. Opt. Soc. Am. B* **24**, 2394–2405 (2007).
22. Y. Sheng, S. M. Saltiel, K. Koynov, "Cascaded third-harmonic generation in single short-range-ordered nonlinear photonic crystal," *Opt. Lett.* **34**, 656–658 (2009).
23. Y. Le Grand, D. Rouede, C. Odiu, R. Aubry, and S. Mattauçh, "Second-harmonic scattering by domains in RbH₂PO₄ ferroelectric," *Opt. Commun.* **200**, 249–260 (2001).

Efficiency of second-harmonic generation (SHG), as well as many other parametric processes, relies on the phase synchronization of the generated and fundamental waves [1]. This, the so-called phase matching condition reflects the conservation of linear momentum of light during the wave interaction. In many nonlinear materials, the phase-matching cannot be naturally satisfied because the material dispersion causes the refractive indices of interacting waves to differ. While a number of techniques can be adopted to achieve phase matching, e.g. temperature and angular tuning in birefringent materials, one of the most successful and universal methods is the so-called quasi-phase matching [1, 2]. It is based on a periodic change of the sign of the nonlinearity with period Λ chosen in such a way that the corresponding reciprocal wave vector $|\vec{G}| = 2\pi/\Lambda$ fulfils the phase matching condition which for SHG reads $2\vec{k}_{(\omega)} + \vec{G} = \vec{k}_{(2\omega)}$, where $\vec{k}_{(\omega)}$, and $\vec{k}_{(2\omega)}$ are the wavevectors of the fundamental (FW) and the second harmonic (SH) beams, respectively. The reversal of the sign of quadratic nonlinearity can be realized in ferroelectric crystals such as lithium niobate or lithium tantalate by periodic poling via application of high voltage. Such high voltage reverses locally the direction of spontaneous polarization of these crystals [3] according to a prescribed pattern. The drawback of this technique is that once fabricated the structure works only for a particular nonlinear process and particular choice of the wavelengths of the interacting waves. To remedy this limitation the quasi-periodic structures or sequences of periodic regions with different periods have been proposed [4–6].

In the 90s, Horowitz *et al.* [7] and Kawai *et al.* [8] demonstrated broadband generation of diffusive-type second-harmonic waves in unpoled strontium barium niobate (SBN) crystals. This emission occurred due to the presence of elongated antiparallel ferroelectric domains (directed along the optical axis) in as grown crystals. Because of the random size and spatial distribution of these domains, the unpoled SBN crystals belong to the class of disordered nonlinear quadratic crystals. Such crystals have attracted a considerable attention in recent years

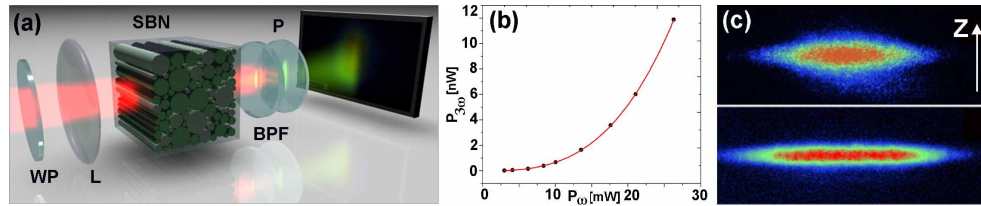


Fig. 1. (a) Schematic of the experimental setup. The multi-domain structure of the SBN sample is schematically shown. L – lens, WP – half wave-plate, BPF – band pass filter, P – polarizer. (b) Power of the third harmonics vs. the input power of the fundamental beam (measured with Ophir Laser Power Head PD300-UV, accuracy $\pm 3\%$). Solid line represents a cubic fit. (c) Experimentally recorded transverse intensity distribution of the second (top) and third (bottom) harmonics.

due to their potential benefits for nonlinear parametric processes [9]. In this particular case the SBN crystal with its spatially random distribution of nonlinearity provides phase matching for second-order nonlinear processes for practically any incident wavelength [10]. The extensive studies of the second-order nonlinear processes in SBN crystals resulted in demonstration of a number of applications including, e.g., multi-frequency conversion [11–13], conical and planar emission [14–16], as well as the frequency mapping from infrared to visible [17]. Recently, it has also been shown that disordered domains in SBN can be used to construct simple autocorrelator for diagnostics of femtosecond pulses [16, 18].

It has been demonstrated previously that periodically poled quadratic nonlinear media can be used in third-harmonic generation (THG). The process is based on cascading of two quadratic effects: SHG followed by sum frequency mixing [19–22]. Because of these two independent processes, two phase matching conditions should be satisfied simultaneously. Obviously, this requires prior knowledge of all involved wavelengths, in order to manufacture a desired structure. However, this is not the case of random quadratic medium which will automatically phase match any parametric process, provided the degree of randomness is high enough. In fact, the first observation of THG in such medium has been reported by Molina *et al.* [10]. However, since the generated signal was very weak only qualitative observation were conducted.

In this work we present, what it is to our knowledge, the first quantitative experimental analysis on cascaded THG in unpoled SBN crystals with disordered ferroelectric domain structure. We discuss the spatial distribution of the generated waves, as well as their polarization properties and compare them with the theoretical model.

In the experiment [see Fig. 1(a)] a linearly polarized fundamental beam from the femtosecond fiber laser (400 fs at $\lambda = 1550\text{nm}$, 5 MHz, 20 kW peak power) passes through a half wave-plate (WP) and is focused by a lens L (8cm focal length) onto the X-face of a sample of unpoled SBN crystal. The input polarization of the beam can be varied from ordinary to extraordinary by adjusting the WP. Band-pass filter (BPF) separates the fundamental beam and its harmonics so their corresponding powers and spatial intensity distribution can be measured and recorded onto a CCD camera from the screen located 22mm behind the crystal. In addition, a polarizer (P) enables measurements of the ordinary and the extraordinary components of the generated harmonics.

When the linearly polarized fundamental beam is launched into the SBN crystal, the SH and third harmonic (TH) beams are readily observed. However, the random character of the ferroelectric domain distribution results in a low conversion efficiency for both harmonics. For an average input power of 27 mW of the fundamental beam, the power of the second and third harmonics are $40\ \mu\text{W}$ and 11 nW, respectively. The plot in Fig. 1(b) depicts the measured dependence of the power of the third harmonic as a function of the power of the fundamental

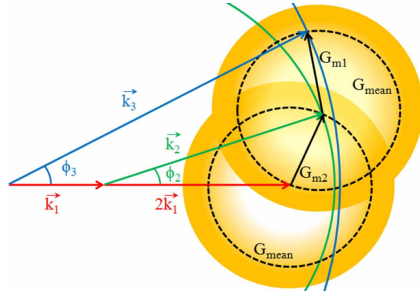


Fig. 2. Diagram of the phase matching for cascaded third harmonic generation in random SBN crystal. Reciprocal vectors G_{m1} and G_{m2} phase match the seconds and third harmonics generation, respectively. Note the broadening of the emission angle for the THG.

beam. As expected, the experimental points follow faithfully the cubic fit (solid red line). It is worth stressing here that in order to determine possible contribution of the direct third harmonic generation via the third order nonlinearity we run a test experiment using a single domain SBN crystal. Since *no third harmonic signal had been detected* under the same experimental conditions we are confident that the observed TH emission in a random domain SBN was indeed a result of the cascaded $\chi^{(2)}$ process.

The images in Fig. 1(c) depict the spatial light intensity distribution of both, SH and TH beams (for an extraordinary polarized fundamental wave). As the emission region is small (hundred microns) compared to the crystal-screen distance, these images represent in fact the far field or spatial spectrum of the emitted waves. It clearly visible that compared to the SH, the TH trace is narrower along the vertical (Z) axis but at the same time broader along the horizontal (Y) axis. While the narrowing of the TH intensity can be attributed to the smaller spatial overlap between the fundamental and the second harmonic waves, the elongated Y-trace is directly related to the domain randomness and its role in the phase matching process. To explain this let us first recall that the formation of the third harmonic is a result of two cascaded quadratic processes: second harmonic generation: $E_{(2\omega)} \propto \hat{d}_{eff}^{(1)} \vec{E}_{(\omega)}^2$ and sum frequency generation in which the third harmonic of the input field is formed by mixing of the fundamental and second harmonic waves: $E_{(3\omega)} \propto \hat{d}_{eff}^{(2)} \vec{E}_{(\omega)} \vec{E}_{(2\omega)}$, where $\hat{d}_{eff}^{(1)}$ and $\hat{d}_{eff}^{(2)}$ represent the effective nonlinearity of the constituent processes.

These processes involve simultaneous fulfillment of two phase matching conditions which are schematically illustrated in Fig. 2. The random domain distribution provides a broad set of reciprocal wavevectors (\vec{G}_m - formally determined by the Fourier spectrum of the domain structure) that are used to phase match the second harmonic generation (Fig. 2). These vectors are represented in the graph by the orange disk with the dashed-line circle representing the mean value of the $|\vec{G}_m|$ distribution. Then the phase matching condition is satisfied in the area of intersection of this disk with a ring representing the spatial direction of the wave-vector of the second harmonic $\vec{k}_{(2\omega)}$. As a result, the generation of the second harmonic is non-collinear with broad spatial distribution of the intensity. The second constituent process involves the interaction between the directed fundamental beam and the already spatially distributed second harmonic. The angular emission of the latter is now determined by the intersection of the big circle (with the radius $|k_{(3\omega)}|$) with a disk of the reciprocal vectors \vec{G}_m . Since the randomness contributes to both cascaded processes by providing the reciprocal \vec{G}_m vectors, the resulting spatial distribution of the generated TH is broader than that of the SH (angle $\phi_3 > \phi_2$). It should be stressed here that because of randomness of nonlinearity the described above generation of SH and TH can be realized for broad spectral range of the fundamental wave. This was confirmed in separate experiments with fundamental wave in the range 1200nm - 1550nm.

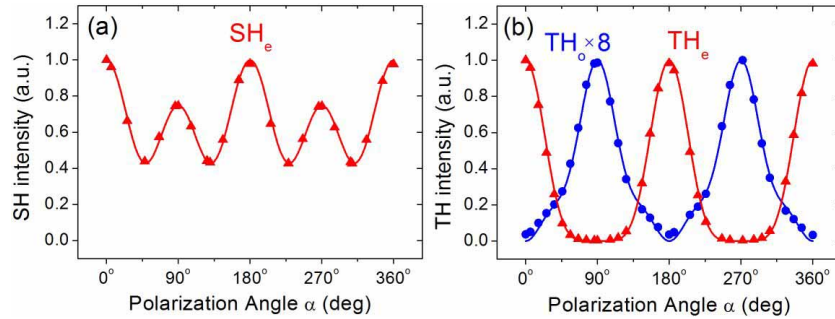


Fig. 3. The power of the ordinary (blue) and extraordinary (red) components of the second (a) and third (b) harmonic as a function of the input polarization angle of the fundamental beam. 0° corresponds to the extraordinary fundamental wave. Points - experimental data; lines - theoretical fit – Eqs.(1-2).

Next we study the polarization properties of the emitted harmonics. To this end, while the azimuthal angle α of the linearly polarized fundamental wave is varied from zero to 360° , the power of both, ordinary and extraordinary components of the SH and TH signals are recorded. The results of this measurement are shown in Fig. 3, where the experimental data is represented by dots and triangles. The graph in Fig. 3(a) shows the power dependence of the extraordinary component of the SH. Interestingly, in our experiments the ordinary component of SH is negligibly weak hence, the SH is always extraordinary polarized. On the other hand, the third harmonic contains both, ordinary and extraordinary components. Their dependence on polarization of the fundamental wave is displayed in Fig. 3(b). Clearly, the strongest SH and TH signals are recorded for an extraordinary fundamental wave. The solid curves in both graphs represent the theoretical predictions which are obtained by considering all possible processes contributing towards the generation of second and third harmonics.

We denote by O_j and E_j the ordinary and extraordinary components of the j -th wave ($j = 1, 2, 3$ for the fundamental, second, and third harmonic, respectively). Then, for arbitrary polarized fundamental wave, the second and third harmonics will, in principle, contain ordinary and extraordinary components. We start with SHG. Its extraordinary component is formed via the following two processes: $E_1E_1 \rightarrow E_2$ and $O_1O_1 \rightarrow E_2$. On the other hand, the ordinary component of the SH is obtained via a single interaction, $E_1O_1 \rightarrow O_2$. The third harmonic is formed due to mixing of photons from the fundamental and second-harmonic beams. In particular, the extraordinary component is created via the processes $E_1E_2 \rightarrow E_3$ and $O_1O_2 \rightarrow E_3$, while the ordinary component appears due to the wave mixing, $E_1O_2 \rightarrow O_3$ and $O_1E_2 \rightarrow O_3$.

The strength of each of these nonlinear processes is determined by the corresponding effective nonlinearity [16]. In homogeneous media, all these processes contribute coherently to the total amplitude of the generated harmonic. However, because of the disorder in the domain distribution, this is no longer the case. As discussed earlier [9], the disorder in a nonlinear crystal leads to the incoherent build up of the generated waves. As a result, the two constituent processes in SHG, namely $E_1E_1 \rightarrow E_2$ and $O_1O_1 \rightarrow E_2$, are mutually incoherent. In fact, such a breakup of mutual coherence between two constituent nonlinear processes has already been noticed in the studies of SHG in random crystals [16]. However, the effect of randomness is even more profound. Since in our experiments only an extraordinary SH component is generated, the effective nonlinearity responsible for the interaction $E_1O_1 \rightarrow O_2$ is negligible. In homogeneous crystals, the effective nonlinearity is directly proportional to the relevant element of the $\chi^{(2)}$ tensor. The situation is more complex in media with random domains. As pointed out by Le Grand *et al.* [23], the randomness generally weakens the strength of nonlinear interactions. Consequently, the constituent interactions involving different polarization states of the

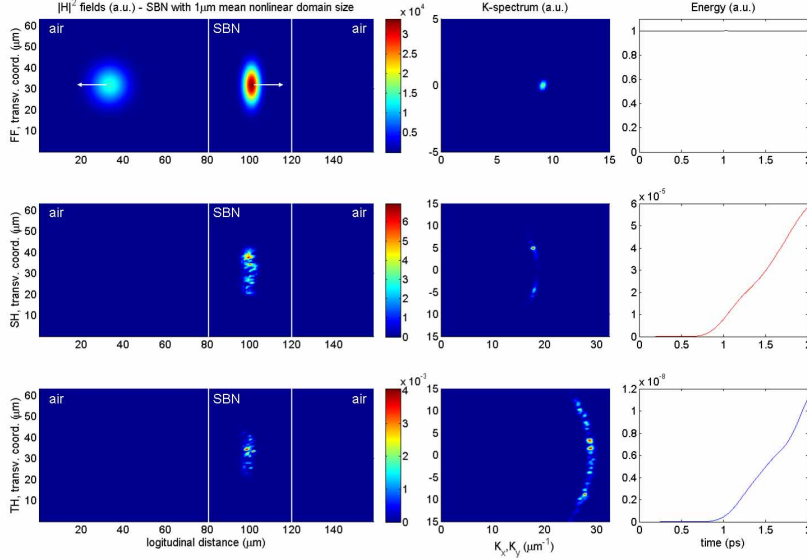


Fig. 4. Numerically results (Media 1). Generation of the second and third harmonics by a femtosecond laser pulse in a disordered structure. Left column: Spatial intensity distribution of the fundamental, second, and third harmonics (from the top to bottom). Middle column- the transverse structure of the interacting waves in the Fourier space. Note the much broader emission angle for the third harmonics. Right column - energy of the fundamental, second, and third harmonics as a function of the time of propagation of the fundamental pulse in the SBN crystal.

fundamental beam and its harmonics will be affected differently by the disorder. Introducing the ordinary and extraordinary intensity components of the fundamental beam as $I_{(\omega)} \cos^2 \alpha$ and $I_{(\omega)} \sin^2 \alpha$, respectively, and taking into account the mutually incoherent character of the contributing nonlinear processes, we present the intensity of the ordinary and extraordinary components of the second and third harmonics by the following relations,

$$I_{(2\omega)}^{(e)} \propto I_{(\omega)}^2 (\cos^4 \alpha + R_1 \sin^4 \alpha), \quad I_{(2\omega)}^{(o)} = 0, \quad (1)$$

$$I_{(3\omega)}^{(e)} \propto I_{(\omega)}^3 (\cos^6 \alpha + R_2 \sin^4 \alpha \cos^2 \alpha), \quad I_{(3\omega)}^{(o)} \propto I_{(\omega)}^3 (\sin^6 \alpha + R_3 \sin^2 \alpha \cos^4 \alpha), \quad (2)$$

where the quantities R_1 , R_2 and R_3 represent relative strengths of the constituent nonlinear processes. They are used as free parameters in fitting the formulas (1-2) to the experimental data, as shown in Fig. 3. We found that the best agreement between experiment and theory is achieved for $R_1 = 0.75$, $R_2 = 0.011$ and $R_3 = 1.1$.

Finally, we study numerically the formation of third harmonic radiation in disordered $\chi^{(2)}$ structure by solving directly the Maxwell equations, assuming the propagation of the fundamental pulse in a two-dimensional nonlinear medium with randomly distributed domains (Gaussian distribution with mean value of $1\mu\text{m}$ and standard deviation of $0.1\mu\text{m}$). The movie in Fig. 4 illustrates the dynamics of the process by depicting the second and third harmonics in a real and Fourier space, respectively. In this way, one can easily capture the spatial properties of the generated waves. The difference in the angular emission for both second and third harmonics is clearly visible. It is worth noting that the same simulations conducted for a single domain crystal (with the same nonlinearity) did not produce any third harmonic signal.

In conclusion, we have studied the third harmonic generation via cascading of two second-order parametric processes in a nonlinear crystal with disordered ferroelectric domains. We

have analyzed a spatial distribution of the intensity of the generated radiation as well as its polarization properties. Our experimental results agree well with the theoretical model incorporating the effect of nonlinearity disorder in the parametric wave interaction.

Acknowledgements

This work was supported by the Australian Research Council, Spanish Government (FIS2008-06024-C03-02), Catalan Government (2009 SGR 1168), and the COST Action MP0702.